Research Article　　　　　　　　　　　　　　　　　　　　　　　**Open Access**

Optical and Degradation Characteristics of Green Synthesized Cornstarch-Base Bioorganic Polymer

Marowa Yass[1], Ahmed Al-Haddad[1]*, Ali Jaafar Sadeq[2]

[1]Department of Physics, College of Science, Mustansiriyah University, 10052 Baghdad, IRAQ.
[2]Applied and Nonlinear Optics Department, Institute for Solid State Physics and Optics, Wigner Research Centre for Physics P.O. Box 49, H-1121 Budapest, Hungary.

*Correspondent contact: ahmed.al-haddad@uomustansiriyah.edu.iq

Abstract

Chemical-base polymers are mostly related to environmental pollution since their poisonous, non-biodegradable wastes, and negatively impact plants, animals, and people. In many locations where petroleum-based plastics are used, bioorganic polymers and biomaterials can play a promising role and are accepted. In one such attempt, glycerol was used as a natural plasticizer, and cornstarch was used to create bioorganic polymers and biocomposites. Resulting in a highly degradable bioorganic polymer in water and soil, display FE-SEM images of a BOP's top and cross-section views, flat surface and smooth, the inner structure of BOP does not demonstrate any bubbles, cracking, flipping, or splitting., estimate the optical band gap indirect of BOP of 3.69 eV that can absorb 96% of UV light and transmit 98 % of visible light. The FTIR assay detects the functional aggregates of the BOP as well as the presence of a hydrogen bond in the BOP matrix. Raman spectroscopy detection composition and scope distribution of the various components in a prepared BOP. The decay constants of BOP were gaged as 12.4 ± 1.8 and 3.49 ± 0.41 for the water and soil, respectively. The decay values show an acceptable variation due to the nature of the BOP on one side and the water and soil on the other side. These findings conclude diverse applications highlighting BOP as a candidate, e.g., UV screening or protective layer, food packaging, and replacing the chemical fertilizer with BOP agent to deliver the organic substances to the plants.

Keywords: Green Synthesis; bioorganic; polymer; optical properties; degradation.

الخلاصة

ترتبط البوليمرات ذات القاعدة الكيميائية والمواد البلاستيكية ذات الاساس النفطي بالتلوث البيئي وذلك بسبب نفاياتها السامة وعدم قابليتها للتحلل مما يؤثر سلبًا على النباتات والحيوانات والإنسان. ويمكن أن تلعب البوليمرات العضوية الحيوية والمواد الحيوية دورًا مهماً وبديل عن المواد البلاستيكية ذات الاصل النفطي . ومن هذه المحاولات لإنشاء بوليمرات عضوية حيوية تم استخدام الجلسرين كمادة ملدنة و نشا الذرة كبوليمر . مما يؤدي إلى وجود بوليمر عضوي حيوي قابل للتحلل بدرجة كبيرة في الماء والتربة، واظهرت صور FE-SEM من الاعلى والمقطع العرضي لـلبوليمر العضوي BOP،ان السطح املس وسلس ولا يُظهر الهيكل الداخلي لـBOP أي فقاعات أو تشقق أو انقسام، وتم تقدير فجوة النطاق البصري غير المباشرة لـBOP البالغة ٣,٦٩ فولتًا والتي يمكنها امتصاص ٩٦٪ من الأشعة فوق البنفسجية ونفاذية ٩٨٪ من الضوء المرئي. ويظهر اختبار FTIR المجاميع الوظيفية لـBOP. اما التحليل الطيفي لرامان فأظهر توزيع نطاق المكونات المختلفة في BOP المُعد. تم قياس ثوابت اضمحلال BOP على أنها ١٢,٤ ± ١,٨ و ٣,٤٩ ± ٠,٤١ للمياه والتربة على التوالي. تظهر قيم الاضمحلال تباينًا مقبولًا بسبب طبيعة BOP من جانب والمياه والتربة من الجانب الآخر. تختتم هذه النتائج بتطبيقات متنوعة تسلط الضوء على BOP كمرشح جيد، على سبيل المثال، فحص الأشعة فوق البنفسجية أو الطبقة الواقية، وتغليف المواد الغذائية، واستبدال الأسمدة الكيماوية ببوليمر عضوي لقابليته العالية على التحلل دون ان يسبب اي مواد خطرة.

INTRODUCTION

Petrochemical-based polymers have a long polymeric chain and are utilized in various applications because of their adaptability and cheap cost, are widely used [1][2]. Petroleum-based plastics have contributed billions to the world economy, yet their non-degradability poses a significant challenge to the ecosystem and has contributed to several environmental problems [3]. The fact that petroleum-based plastics are not

biodegradable or easily broken down makes them a major ecological problem. Therefore, finding sustainable replacements for these products is an immediate priority [4][5].

Biodegradable plastics, which may be manufactured from either naturally occurring bioorganic polymer (BOP) or synthetic bio-based polymer, appear to be a viable option to completely replace or significantly reduce the reliance on conventional plastics and the pollution they produce [6][7]. Furthermore, BOP originating from renewable resources like animals and plants can resolve the environmental issues related to the rising usage of petroleum-based plastics and the difficulty brought on by the depletion of oil reserves, Natural fabrics, cellulose, polysaccharides, proteins, lipopolysaccharides, polyhydroxyalkanoates, and glycolipids are all examples of BOP that can be used for ecological purposes [8][9]. Because of their versatility and functional properties, including low density, excellent absorption capacity, gas, biodegradability, water vapour, and lipid permeability, BOP offers a viable alternative to traditional plastics. They have several applications in many industries, including agriculture, medicine, packaging, food service, textiles, etc., [10].

Starch is the most commonly utilized in BOP production for its high optical performance, high degradation, and the main ingredient in almost half of all commercially available BOP [11]. In addition to their widespread use in packaging, the production procedure of the starch-based BOP is not complicated. Starch's tensile qualities make it ideal for use in the manufacturing of packing materials. The majority of plant species synthesize this polysaccharide. This carbohydrate is a vital part of the human diet and can be found in massive quantities in staple foods including cassava, rice, maize (corn), potatoes, wheat, etc. A large number of glucose molecules linked together by glycosidic bonds characterize the carbohydrate known as starch. Corn starch was used to create a biodegradable polymer with tunable surface properties starch powder non-toxic, tastes, smells neutral, and semi-permeable to biological and carbon dioxide. Starch contains both of helical and linear amylose and branching amylopectin [12]. Depending on the plant, amylose ranges from 20–25% and Amylopectin from 75–80% by weight; Amylopectin dwarfs amylose. Starch swells and bursts when heated. The semi-crystalline structure is destroyed, and small amylose particles percolate out of the granule to create a network [13]. Glycerol is typically mixed with the starch to give it a more malleable texture. The BOP desired properties can be engineered by adjusting the amounts of the additives used [14]. Increasing the amylose content of the bioplastics would improve their tensile qualities [15]. Ghanbarzadeh *et al.* found that the films made based on pure starch are brittle and fragile, especially compared to films made from cornstarch, which has a lower concentration of amylose content [16]. D. Amalia *et al.* In (2020) He used cornstarch derived from corn and ground corn husk as base material and filler, respectively to improve the mechanical properties of bioplastic [17]. M. K. Maricela *et al.* In (2019) studied BOP based on rice starch and cornstarch packaging applications, various bioplastic films are synthesized with diverse formulations such as starch, gelatin, citric acid, and glycerin. In addition flexibility of the BOP could be improved by adding rice and cornstarch [18].

To overcome petrochemicals pollution, we demonstrate cornstarch-based BOP preparation with large-scale and simple manufacturing. The optical properties confirm the BOP's capability to be involved in diverse applications such as food packaging, UV protective layer, UV screening, and even could replace the chemical fertilizer as a good agent (highly degradable agent in water and soil) to deliver the organic substances to the plants.

MATERIALS AND METHODS

The chemicals in this investigation were purchased from Sigma Aldrich and were of analytical purity; no additional processing was performed on them; the fine powder of cornstarch was purchased from a local supermarket.

BOP Synthesization

First of all, 1 g of fine powder of cornstarch was added to a beaker containing 25 ml of DI-H_2O, then, 0.4 ml of CH_3COOH (vinegar) and 0.6 ml of $C_3H_8O_3$ (glycerol) were merged [19]. The mixture was stirred for 10 minutes, as illustrated in Figure 1a, secondly, the whole mixture was localized on a hot-plate stirrer at 80 °C for 45 minutes to polymerize the solution, as shown in Figure 1b. The resulting BOP shows a significant increase in viscosity. A solution-casting technique was used to apply the BOP solution on a petri dish (10 cm) and

allowed it to cool down at room temperature before drying the thick films for 16 hours at 60°C (Figure 1c). Finally, the thick layer of BOP was divided into 18 samples with dimensions of (1×1 cm^2) and stored in a tightly closed glass container at room temperature. The degradation investigation was carried out for 9 samples in the water with a pH value of 7, meanwhile, the other 9 samples were placed into dried soil with an average humidity value of around 60 %. Every 48 hours, one sample is taken out either from water or soil and then recording the thickness change.
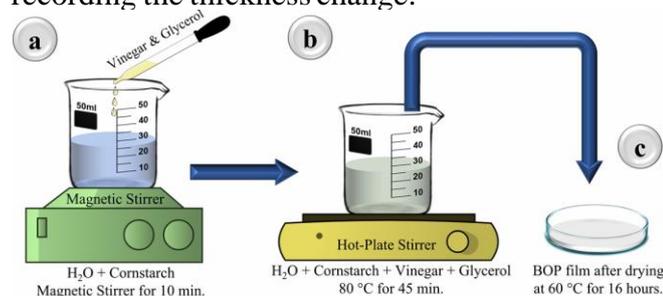

Figure 1. Schematic of cornstarch-based BOP fabricating, a) adding vinegar and glycerin to the glass container with a mixture consisting of DI water and fine powder of cornstarch; b) Heating the entire mixture of step A at 80 °C in a hot-plate stirrer for 45 minutes, c) Transfer the dense solution of BOP into a petri dish and dry it.

Overall, the solution-casting technique for BOP production in this study provides a facile and effective technique for BOP thick layer generation and enhanced the mechanical endurance that is sufficient to handle all the experimental conditions.

Instrumentations and Techniques

An accumulation of BOP prepared by solution-casting technique was examined using a field-emission scanning electron microscopy (FE-SEM, Inspect F-50 SEM). Additionally, Raman spectrometer type in Via^{TM} was involved to analyze the POB sample with a laser (532 nm), 1800 grating, at 50x objective using 10% of laser power, 25 accumulated, and 1 s of exposure time during the measurement. Moreover, Fourier-transform infrared (FTIR) spectroscopy (BURKER) in the range of 4000 cm^1 to 500 cm^1 was contributed to identify the functional groups in the BOP. Furthermore, the optical properties of BOP were examined using a UV spectrophotometer type T70/T80 series UV/Vis Spectrometer. Thereafter, using a Digital Micrometer accurate to within 1 µm, the average film thickness was determined for

Bioplastics obtained and tested for thickness. Water solubility and soil degradation for analysis through thickness decrease.

RESULTS AND DISCUSSION
Morphology and Structural

Figure 2a and 2b displays FE-SEM images of top and cross-section views of a BOP, respectively, prepared by dropping the dense solution onto a glass substrate. the results of BOP present a smooth and flat surface of a large area of the BOP. In addition, the inner structure of BOP does not demonstrate any bubbles, cracking, flipping, or splitting. Moreover, the BOP shows a high stability at 60°C through preparation conditions that could be evidence for BOP constancy in extreme environmental circumstances.

Figure 2c shows the FTIR spectrum with a broad transmission peak at 3280 cm^{-1} as a functional hydroxyl group in the BOP. The C-H bonds at 2927, 2880 cm^{-1}, and C=C bond at 1646 cm^{-1} explain the presence of carbonyl glucose in starch as similar to C-H bond at 1416, 1347 cm^{-1}. Besides, C-O bond was consisted at 1152,1078, and 1026 cm^{-1} with formation of C-H bonding at 924 cm^{-1}, 846 cm^{-1}, and 757 cm^{-1}, respectively. The C=C, and C-H, bonding may strong relation in increasing the FTIR spectrum of the BOP, the difference of peaks intensity and width related with purity and mixing ratio of the components. Glycerol contains an O-H group with C-H alkanes. In addition, the increases of the peak width and intensity of the stretching O-H group are due to physical strength and degradation of the BOP, revealing an interaction between the hydroxyl groups of starch and glycerol that cause [20-22].

All major vibration types are predicted in the spectrum between 200 and 2000 cm^{-1} of the Raman shift spectrum of the various BOP, Figure 2d. The value of peak position is not identical for all components due to the variant of the chemical structures since the bonds of chemicals involved in the structure of polymers are different. We found two peaks for BOP at 252 and 483 cm^{-1}, which were attributed to the bending of vibrations over the C-C banding and oxygen backbones [23]. The weak carbonyl group at C-C was attributed to the peak at 871 cm^{-1} and the peak at 1068 cm^{-1} was attributed to polyethylene

C-C bending vibration [23, 24], at higher wavenumbers. Lastly, CH$_3$-CH$_2$ deformation was linked to a high point at 1460 cm^{-1}. These results offer deep insights into the composition and band distribution of the different components in the prepared BOP.
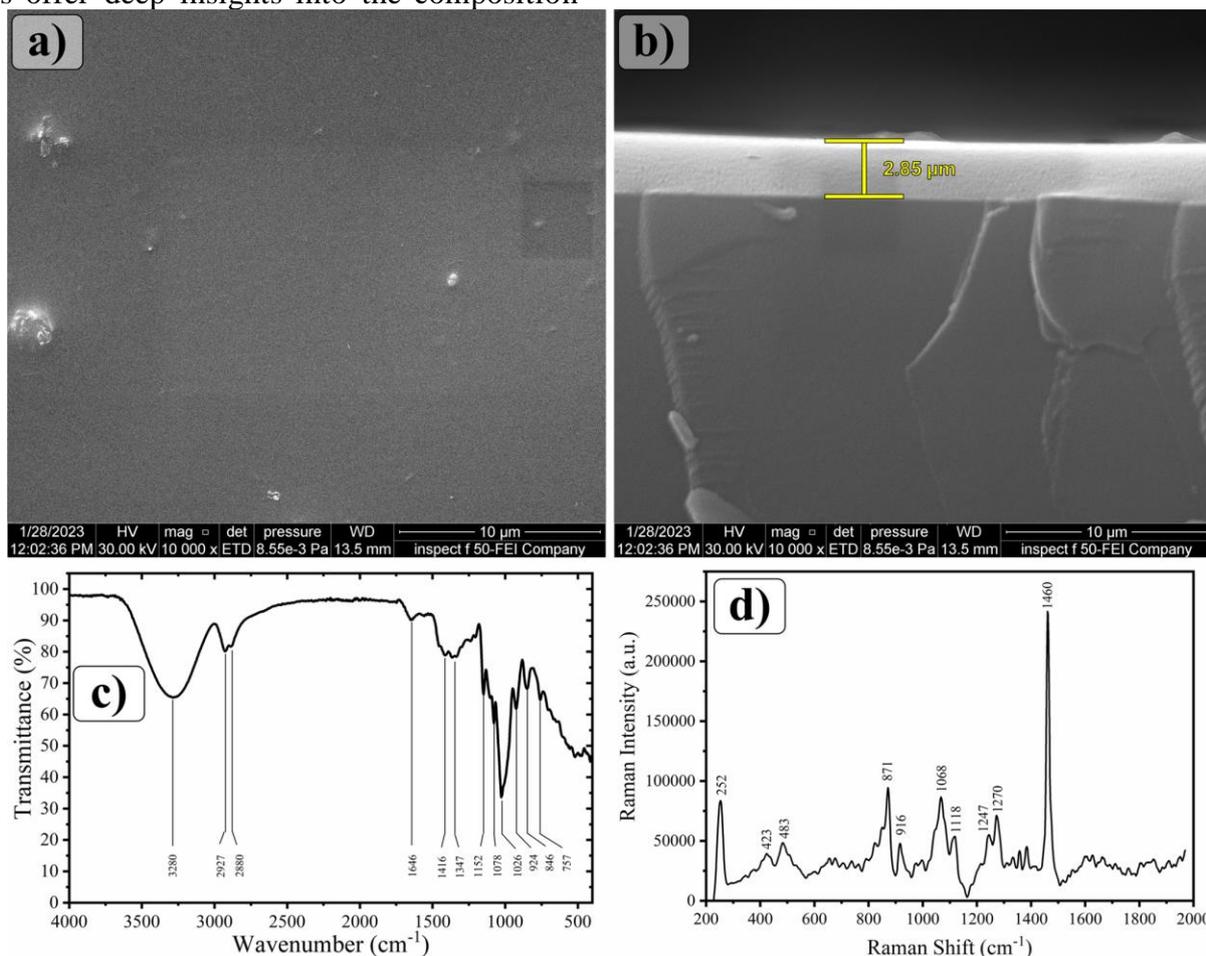

Figure 2. FE-SEM analysis of BOP: a) top view of a large area of BOP; b) Cross-section view of BOP, c) FTIR Spectrum of BOP, d) Raman spectrum of BOP.

Optical Parameters

The ultraviolet-visible (UV-Vis) absorbance spectrum of the BOP is shown in Figure 3. The UV-Vis spectrophotometer was utilized to determine the absorbance and the transmittance of BOP 200 and 1000 nm, in order to establish studying the optical properties of the created thick layer of BOP (the inset photo in Figure 3). A beam of UV-Vis light incident perpendicularly on the BOP thick film. This investigation outcome spotting the film's transparency and UV-screening qualities, which are crucial for uses like packaging, solar cells, and bio-optical coating [25]. However, the thick BOP layer absorbance peak displayed a prominent peak at 330 nm in wavelength. The height of the absorption peak of 0.96 a.u, which denotes an increase in BOP transparency, was noted which indicates the fact of susceptibility of BOP to photo-degradation and UV energy absorption.

There is no doubt about the great transmittance (98 %) of the thick film of BOP at the visible region (longer than 400 nm), suggesting their application in an UV light protective and visible light transparent window, which is consistent with the optical characteristics of BOP in the UV-Vis range. However, when the wavelength is below 400 nm, there is a significant decrease in the film's transmittance (referring to the cut-off region), which is caused by the high absorbance of the film at this region.

Further, the absorption coefficient (α) can be calculated through the equation [26]:

$$\alpha = \frac{2.303 \times A}{l} \qquad (1)$$

in which *A* and *l* are the absorbance and the thickness of BOP, respectively.

In general, the prepared BOP could have either indirect or direct transitions. Therefore, we preferentially estimate both types of transitions to

estimate the optical band gap (E_g) of the BOP by using Tauc's relation [27]:

$$(\alpha h\gamma) = A(h\gamma - E_g)^r \qquad (2)$$

in which $h\gamma$ is the photon energy, r is an integer depend on electronic transition, for direct transition is equal 1\2 and for indirect transition is equal 2.
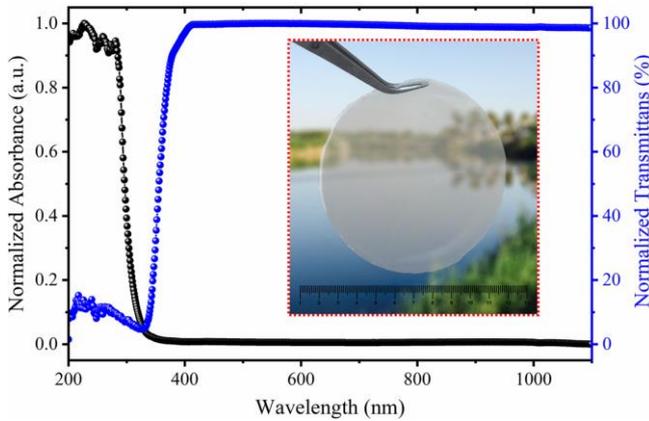

Figure 3. Normalized absorbance and transmittance spectrum of BOP; the inset represents photographs of a thick layer of large area BOP (10 cm diameter).

As shown in Figure 4a, once the transition is direct, the calculated value of the E_g is 4.11 eV, and if the transition is indirect, the E_g will be valued as 3.69 eV. Accordingly, The BOP has an indirect optical band gap [28].

Figure 4b demonstrates the refractive index and extinction coefficient (k) as a function of the wavelength and their corresponding photon energy. Due to the high lattice resonance within wavelength around 200 to 250 nm, the refractive index is valued as maximum as ~ 4[29]. The refractive index is related with light velocity and the density of material [30], Figure 4b clearly displays the dependence of the refractive index of BOP on photon energy, which rises with photon energy increase and vice versa.

High refractive index polymers can be utilized in medical lens applications to help shrink the curvature of the lens by allowing light to bend more within the material. Additionally, when the refractive index rises, the lens thickness falls, reducing weight. The value of the refractive index may be utilized to package food using this increase[31][32].

In the presence of transmittance (T), the refractive index (n) can be estimated by using the following equation]33[:

$$n = \frac{1}{T} + \sqrt{\frac{1}{T-1}} \qquad (3)$$

Extinction coefficient is the inertia that occurs in the electromagnetic wave, i.e., the number of electrons absorbed from the energy of the incident photons. A low and smooth extinction coefficient at the low photon energy region was observed, while it raises and variant at high energy due to the loss in the energy or could be an indication for the transformation of most of the absorbed photon energy to heat [34].

In other vision, the extinction coefficient decreases with increasing wavelength, which explains the similarity in the behavior of the absorption coefficient as a result of extinction coefficient dependence on absorption coefficient as represented in equation 4 [35].

The following equation can be applied to calculate the extinction coefficient (k) [35]:

$$k = \frac{\alpha\lambda}{4\pi} \qquad (4)$$

Generally, the dielectric constant is distinguished for each specific material, it represents the dielectric losses by the complex number as the imaginary part (ε_i) and it represents the polarization degree of material by the real part (ε_r). The real and the imaginary parts of the dielectric constant could be estimated by using the equations [36]:

$$\varepsilon_i = n^2 - k^2 \qquad (5)$$
$$\varepsilon_r = 2nk \qquad (6)$$

Figure 4c shows the change of the real and imaginary parts of the dielectric constant as a function of wavelength. Both parts of the dielectric constant increase gradually and then begin to decrease with increasing wavelength. However, the variation between both values, nevertheless, this behavior is somewhat similar to the behavior of the refractive index curve due to the dependence of the dielectric constant on the refractive index.

Optical conductivity (σ) is the increase in the number of charge carriers (electrons or holes) due to the incident beam of light. It is clear from Figure 4d. That the optical conductivity values gradually increase with the increase of photon energy, and this is the behavior of the absorption coefficient because of its association with optical conductivity, as represented in the equation [37]:

$$\sigma = \frac{\alpha n c}{4\pi} \qquad (7)$$

The loss tangent (tanδ) is affected by the particle size, and lattice strain, it is determined by using the equation [38]:

$$tan\delta = \frac{\varepsilon_i}{\varepsilon_r} \qquad (8)$$

It is clear that the loss tangent decreases by increasing the real part of the dielectric constant with increasing photon energy as revealed in Figure 4d.
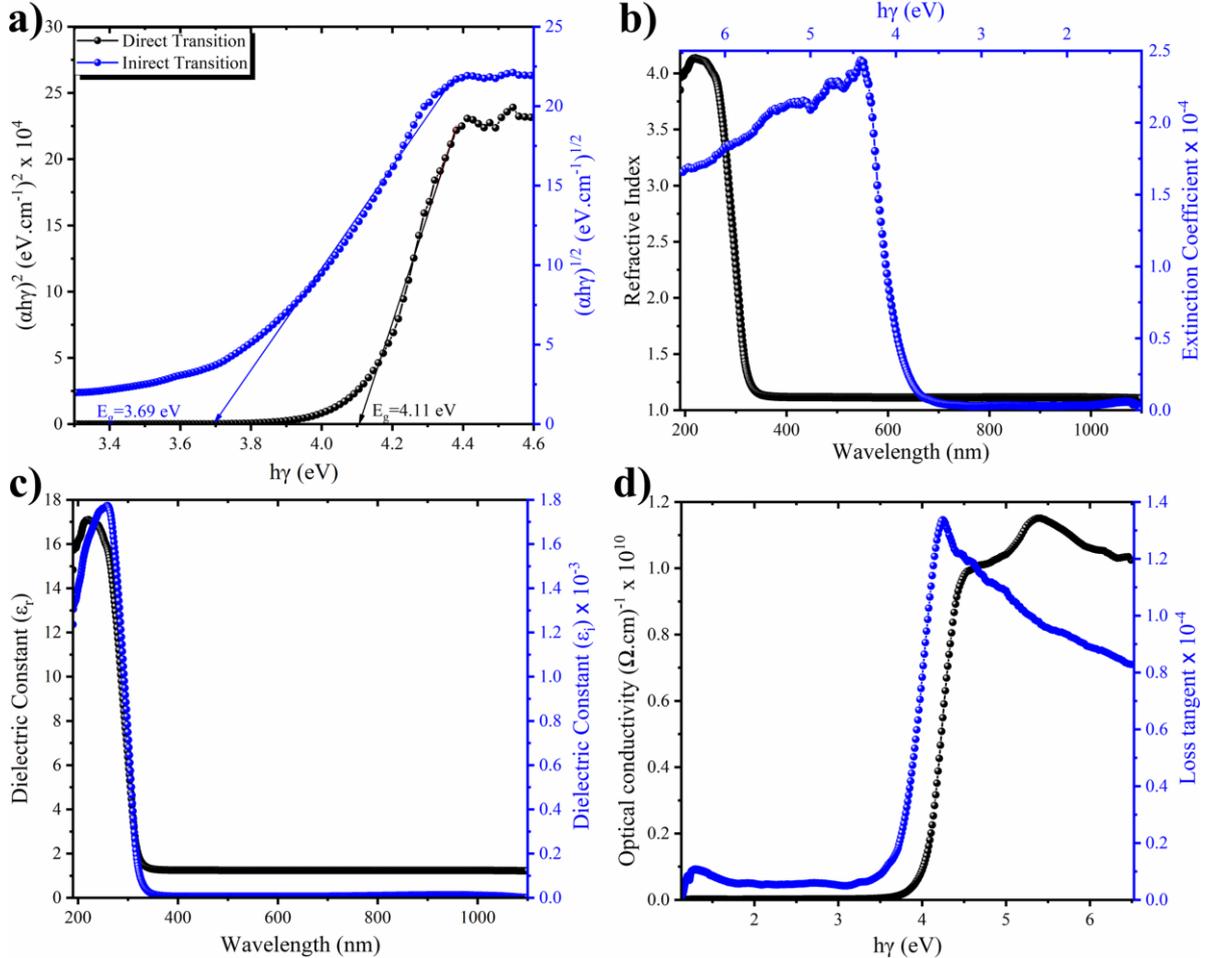

Figure 4. (a) Touc's plot method to estimate the optical band gap (direct and indirect) of BOP (b) refractive index and extinction coefficient of BOP, (c) both parts of dielectric constant the real and the imaginary, (d) optical conductivity and loss tangent of BOP.

The rate of the prepared film of BOP degradation in DI water and soil is demonstrated in Figure 5. Obviously, the BOP degraded in both water and soil with a clear variation, and the BOP samples were smooth and soft texture before placing it into the water. Nevertheless, we noticed changes in color and shape, folding, twisting, and hardness as well as thickness decreasing with each sample after 2 days apart of testing (the above inset photos in Figure 5). These findings indicate chemical changes and dissolving in water resulting in a thickness decrease. Meanwhile, for the sample placed in the soil, we noticed color changes as an indication to decomposition process that occurs in bioplastics with soil, meanwhile the samples consistent with their shape (the bottom inset photos in Figure 5), and a dramatical thickness decrease in

the first three samples. These results also verify the BOP degradation in the soil as a conclusion of the thickness decreasing [39]. Table 2 represents the thickness change of BOP in water and soil for every two days, every 48 hours one sample form water and soil are taken out and measuring their thicknesses and observed the thickness change. The last samples that taken out after day 18 in the water reached to 40 µm thickness, while in the soil, its thickness reached to 60 µm, which indicates the speed of decomposition in the water faster than soil. To evaluate the degradation constant of this experiment, with the increase of days, thickness presents a decay feature. The exponential-decay model ($y/y_o = Ae^{(-\omega \backslash \tau)}$) could be applied to estimate the decay constant (τ), in which y is the thickness, A is a constant, and ω is the days

number. To fit both curves (in water and soil), decay constants were 12.4 ± 1.8 and 3.49 ± 0.41 for the water and soil, respectively. The values show an acceptable variation due to the nature of the BOP in one side and the water and soil on another side. As a result, BOP could replace chemical fertilizer as a good agent (high degradation in water and soil) to deliver the organic substances to the plants. By increasing the number of days of its stay in the soil, as shown in Table 1. The decomposition of bioorganic polymer can be calculated through the following equation.

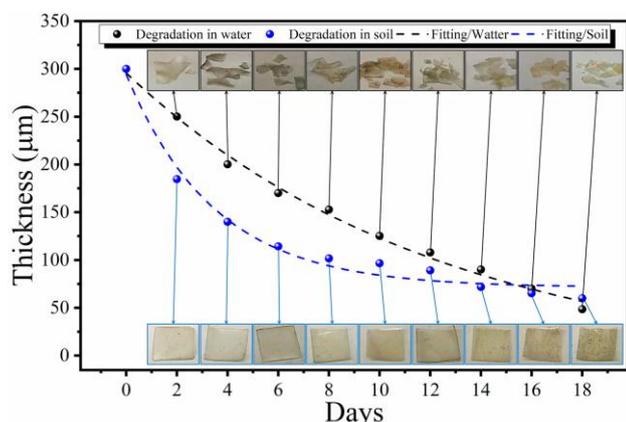$$y = y° + e^{(-x \backslash t)} \tag{9}$$

Figure 5. A number of days as a function degradation of BOP. The blue fitting curve represents the BOP decays in soil and the black fitting curve represents the BOP decays in water.

Table 1. Degradation of a thick layer of BOP in water and soil per day.

days	BOP Thickness (µm)	
	Water	**Soil**
2	250	170
4	200	140
6	170	130
8	160	120
10	130	110
12	120	100
14	90	90
16	70	70
18	40	60

CONCLUSIONS

In the study, cornstarch-based BOP with large-scale manufacture was prepared. The optical characteristics (high UV light absorbed at wavelength lower than 330 nm and high transmittance in visible light 98%), show the ability of prepared BOP to play a crucial role in diverse applications such as food packaging, UV protective layer, and UV screening. Both direct and indirect optical band gap were estimated 4.11 eV and 3.69 eV, respectively. The decay constants of BOP were 12.4 ± 1.8 and 3.49 ± 0.41 for the water and soil, respectively. The decay values show an acceptable variation due to the nature of the BOP on one side and the water and soil on the other side. In advance, the prepared BOP could replace the chemical fertilizer as a good agent (high degradable agent in water and soil) to deliver the organic substances to the plants. Moreover, we still need to find commercially biodegradable plastics made from bioorganic materials instead of petrochemicals to decrease pollution and reduce the oil request. BOP is seen as a good solution to environmental pollution by turning it into compost.

Acknowledgments

References

[1] R. Ilyas and S. Sapuan, "Biopolymers and biocomposites: chemistry and technology," Current Analytical Chemistry, vol. 16, no. 5, pp. 500-503, 2020. https://doi.org/10.2174/1573411016052006030953111

[2] M. Harussani, S. Sapuan, U. Rashid, A. Khalina, and R. Ilyas, "Pyrolysis of polypropylene plastic waste into carbonaceous char: Priority of plastic waste management amidst COVID-19 pandemic," Science of The Total Environment, vol. 803, p. 149911, 2022. https://doi.org/10.1016/j.scitotenv.2021.149911

[3] M. Ilyas, W. Ahmad, H. Khan, S. Yousaf, K. Khan, and S. Nazir, "Plastic waste as a significant threat to environment-a systematic literature review," Reviews on Environmental Health, vol. 33, no. 4, pp. 383-406, 2018. https://doi.org/10.1515/reveh-2017-0035

[4] J. Tarique, S. Sapuan, A. Khalina, S. Sherwani, J. Yusuf, and R. Ilyas, "Recent developments in sustainable arrowroot (Maranta arundinacea Linn) starch biopolymers, fibres, biopolymer composites and their potential industrial applications: A review," Journal of Materials Research and Technology, vol. 13, pp. 1191-1219, 2021. https://doi.org/10.1016/j.jmrt.2021.05.047

[5] N. Nurazzi et al., "Mechanical performance and applications of CNTs reinforced polymer composites-a review," Nanomaterials, vol. 11, no. 9, p. 2186, 2021. https://doi.org/10.3390/nano11092186

[6] A. George, M. Sanjay, R. Srisuk, J. Parameswaranpillai, and S. Siengchin, "A comprehensive review on chemical properties and applications of biopolymers and their composites," International Journal of Biological Macromolecules, vol. 154, pp. 329-338, 2020. https://doi.org/10.1016/j.ijbiomac.2020.03.120

[7] T. M. Bernaerts, L. Gheysen, I. Foubert, M. E. Hendrickx, and A. M. Van Loey, "The potential of microalgae and their biopolymers as structuring ingredients in food: A review," Biotechnology Advances, vol. 37, no. 8, p. 107419, 2019. https://doi.org/10.1016/j.biotechadv.2019.107419

[8] M. Harussani, S. Sapuan, U. Rashid, and A. Khalina, "Development and characterization of polypropylene waste from personal protective equipment (PPE)-derived char-filled sugar palm starch biocomposite briquettes," Polymers, vol. 13, no. 11, p. 1707, 2021. https://doi.org/10.3390/polym13111707

[9] M. N. F. Norrrahim et al., "Greener pretreatment approaches for the valorisation of natural fibre biomass into bioproducts," Polymers, vol. 13, no. 17, p. 2971, 2021. https://doi.org/10.3390/polym13172971

[10] R. L. Reddy, V. S. Reddy, G. A. J. I. J. o. E. T. Gupta, and A. Engineering, "Study of bio-plastics as green and sustainable alternative to plastics," International Journal of Emerging Technology and Advanced Engineering Materials, vol. 3, no. 5, pp. 76-81, 2013.

[11] R. Ilyas et al., "Effect of hydrolysis time on the morphological, physical, chemical, and thermal behavior of sugar palm nanocrystalline cellulose (Arenga pinnata (Wurmb.) Merr)," Textile Research Journal, vol. 91, no. 1-2, pp. 152-167, 2021. https://doi.org/10.1177/0040517520932393

[12] H. R. Kim, S. J. Choi, H.-D. Choi, C.-S. Park, and T. W. Moon, "Amylosucrase-modified waxy potato starches recrystallized with amylose: The role of amylopectin chain length in formation of low-digestible fractions," Food chemistry, vol. 318, p. 126490, 2020. https://doi.org/10.1016/j.foodchem.2020.126490

[13] Y. Zhong et al., "Different genetic strategies to generate high amylose starch mutants by engineering the starch biosynthetic pathways," Carbohydrate Polymers, p. 119327, 2022. https://doi.org/10.1016/j.carbpol.2022.119327

[14] Z. Y. Ben, H. Samsudin, and M. F. Yhaya, "Glycerol: Its properties, polymer synthesis, and applications in starch based films," European Polymer Journal, p. 111377, 2022. https://doi.org/10.1016/j.eurpolymj.2022.111377

[15] A. A. Gabriel, A. F. Solikhah, and A. Y. Rahmawati, "Tensile strength and elongation testing for starch-based bioplastics using melt intercalation method: a review," in Journal of Physics: Conference Series, 2021, vol. 1858, no. 1, p. 012028: IOP Publishing. https://doi.org/10.1088/1742-6596/1858/1/012028

[16] B. Ghanbarzadeh, H. Almasi, and A. A. Entezami, "Improving the barrier and mechanical properties of corn starch-based edible films: Effect of citric acid and carboxymethyl cellulose," Industrial Crops Products, vol. 33, no. 1, pp. 229-235, 2011. https://doi.org/10.1016/j.indcrop.2010.10.016

[17] D. Amalia, D. Saleh, and E. Djonaedi, "Synthesis of biodegradable plastics using corn starch and corn husk as the fillers as well as chitosan and sorbitol," in Journal of physics: conference series, 2020, vol. 1442, no. 1, p. 012007: IOP Publishing. https://doi.org/10.1088/1742-6596/1442/1/012007

[18] M. Marichelvam, M. Jawaid, and M. Asim, "Corn and rice starch-based bio-plastics as alternative packaging materials," Fibers, vol. 7, no. 4, p. 32, 2019. https://doi.org/10.3390/fib7040032

[19] M. I. Din, R. Sehar, Z. Hussain, R. Khalid, and A. T. Shah, "Synthesis of biodegradable semolina starch plastic films reinforced with biogenically synthesized ZnO nanoparticles," Inorganic and Nano-Metal Chemistry, vol. 51, no. 7, pp. 985-994, 2021. https://doi.org/10.1080/24701556.2020.1813768

[20] J. Wang, S. Song, S. Gao, R. Muchakayala, R. Liu, and Q. Ma, "Mg-ion conducting gel polymer electrolyte membranes containing biodegradable chitosan: Preparation, structural, electrical and electrochemical properties," Polymer Testing, vol. 62, pp. 278-286, 2017. https://doi.org/10.1016/j.polymertesting.2017.07.016

[21] Saiful, H. Helwati, S. Saleha, and T. Iqbalsyah, "Development of bioplastic from wheat Janeng starch for food packaging," in IOP Conference Series: Materials Science and Engineering, 2019, vol. 523, no. 1, p. 012015: IOP Publishing. https://doi.org/10.1088/1757-899X/523/1/012015

[22] C. Ma, Z. Ren, Z. Zhang, J. Du, C. Jin, and X. Yin, "Development of simplified models for nondestructive testing of rice (with husk) protein content using hyperspectral imaging technology," Vibrational Spectroscopy, vol. 114, p. 103230, 2021. https://doi.org/10.1016/j.vibspec.2021.103230

[23] P. B. Smith, A. Leugers, S. Kang, S. L. Hsu, and X. Yang, "An analysis of the correlation between structural anisotropy and dimensional stability for drawn poly (lactic acid) films," Journal of Applied Polymer Science, vol. 82, no. 10, pp. 2497-2505, 2001. https://doi.org/10.1002/app.2100

[24] Ł. Łopusiewicz, F. Jędra, and M. Mizielińska, "New poly (lactic acid) active packaging composite films incorporated with fungal melanin," Polymers, vol. 10, no. 4, p. 386, 2018. https://doi.org/10.3390/polym10040386

[25] M. Peydayesh, M. Bagnani, and R. Mezzenga, "Sustainable bioplastics from amyloid fibril-biodegradable polymer blends," ACS Sustainable and Chemistry Engineering, vol. 9, no. 35, pp. 11916-11926, 2021. https://doi.org/10.1021/acssuschemeng.1c03937

[26] K.-Y. Yoon, J. H. Byeon, J.-H. Park, and J. Hwang, "Susceptibility constants of Escherichia coli and Bacillus subtilis to silver and copper nanoparticles," Science of the Total Environment, vol. 373, no. 2-3, pp. 572-575, 2007. https://doi.org/10.1016/j.scitotenv.2006.11.007

[27] A. Al-Haddad et al., "Dimensional dependence of the optical absorption band edge of TiO2 nanotube arrays beyond the quantum effect," The Journal of Physical Chemistry C, vol. 119, no. 28, pp. 16331-16337, 2015. https://doi.org/10.1021/acs.jpcc.5b02665

[28] S. M. Katalenich and M. Z. Jacobson, "Toward battery electric and hydrogen fuel cell military vehicles for land, air, and sea," Energy, vol. 254, p. 124355, 2022. https://doi.org/10.1016/j.energy.2022.124355

[29] G. Ghosh, "Sellmeier coefficients and dispersion of thermo-optic coefficients for some optical glasses," Applied optics, vol. 36, no. 7, pp. 1540-1546, 1997. https://doi.org/10.1364/AO.36.001540

[30] Y. Zhao et al., "Monocrystalline CdTe solar cells with open-circuit voltage over 1 V and efficiency of 17%," Nature Energy, vol. 1, no. 6, pp. 1-7, 2016. https://doi.org/10.1038/nenergy.2016.67

[31] M. F. Maitz, "Applications of synthetic polymers in clinical medicine," Biosurface and Biotribology, vol. 1, no. 3, pp. 161-176, 2015. https://doi.org/10.1016/j.bsbt.2015.08.002

[32] L. M. Shaker, W. K. Al-Azzawi, A. Al-Amiery, M. S. Takriff, and W. N. R. Wan Isahak, "Highly transparent antibacterial hydrogel-polymeric contact lenses doped with silver nanoparticles," Journal of Vinyl and Additive Technology, 2023. https://doi.org/10.1002/vnl.21995

[33] T. Subramanyam, B. Srinivasulu Naidu, and S. Uthanna, "Physical properties of zinc oxide films prepared by dc reactive magnetron sputtering at different sputtering pressures," Crystal Research and Technology, vol. 35, no. 10, pp. 1193-1202, 2000. https://doi.org/10.1002/1521-4079(200010)35:10<1193::AID-CRAT1193>3.0.CO;2-6

[34] Z. G. Zhang and Y. Li, "Polymerized small-molecule acceptors for high-performance all-polymer solar cells," Angewandte Chemie International Edition, vol. 60, no. 9, pp. 4422-4433, 2021. https://doi.org/10.1002/anie.202009666

[35] F. H. Siyanaki, H. R. Dizaji, M. H. Ehsani, and S. Khorramabadi, "The effect of substrate rotation rate on physical properties of cadmium telluride films prepared by a glancing angle deposition method," Thin Solid Films, vol. 577, pp. 128-133, 2015. https://doi.org/10.1016/j.tsf.2015.01.066

[36] J. Tripathi, S. Tripathi, J. Keller, K. Das, and T. Shripathi, "Degradation study on structural and optical properties of annealed Rhodamine B doped poly (vinyl) alcohol films," Polymer Degradation and Stability, vol. 98, no. 1, pp. 12-21, 2013. https://doi.org/10.1016/j.polymdegradstab.2012.11.003

[37] G. S. Ahmed and B. K. Al-Maiyaly, "Annealing effect on characterization of nano crystalline SnSe thin films prepared by thermal evaporation," in AIP Conference Proceedings, 2019, vol. 2123, no. 1, p. 020074: AIP Publishing LLC. https://doi.org/10.1063/1.5117001

[38] K. Urmila, T. Namitha, J. Rajani, R. Philip, and B. Pradeep, "Optoelectronic properties and Seebeck coefficient in SnSe thin films," Journal of Semiconductors, vol. 37, no. 9, p. 093002, 2016. https://doi.org/10.1088/1674-4926/37/9/093002

[39] A. Krishnamurthy and P. Amritkumar, "Synthesis and characterization of eco-friendly bioplastic from low-cost plant resources," SN Applied Sciences, vol. 1, no. 11, p. 1432, 2019. https://doi.org/10.1007/s42452-019-1460-x

How to Cite